Sumoylation inhibits α-synuclein aggregation and toxicity

Petranka Krumova,[1] Erik Meulmeester,[2] Manuel Garrido,[1] Marilyn Tirard,[3] He-Hsuan Hsiao,[4] Guillaume Bossis,[2] Henning Urlaub,[4,6] Markus Zweckstetter,[5,7] Sebastian Kügler,[1,7] Frauke Melchior,[2,8] Mathias Bähr,[1,7] and Jochen H. Weishaupt[1,7]

[1]Department of Neurology and [2]Department of Biochemistry I, University of Göttingen, 37073 Göttingen, Germany
[3]Department of Molecular Neurobiology, Max Planck Institute for Experimental Medicine, 37075 Göttingen, Germany
[4]Bioanalytical Mass Spectrometry Group and [5]Department of Nuclear Magnetic Resonance–Based Structural Biology Group, Max Planck Institute for Biophysical Chemistry, 37077 Göttingen, Germany
[6]Bioanalytical Mass Spectrometry Group, Department of Clinical Chemistry, Göttingen Medical University, 37075 Göttingen, Germany
[7]German Research Foundation Research Center for Molecular Physiology of the Brain, 37075 Göttingen, Germany
[8]Center for Molecular Biology Heidelberg, German Cancer Research Center–Center for Molecular Biology Heidelberg Alliance, 69120 Heidelberg, Germany

Posttranslational modification of proteins by attachment of small ubiquitin-related modifier (SUMO) contributes to numerous cellular phenomena. Sumoylation sometimes creates and abolishes binding interfaces, but increasing evidence points to another role for sumoylation in promoting the solubility of aggregation-prone proteins. Using purified α-synuclein, an aggregation-prone protein implicated in Parkinson's disease that was previously reported to be sumoylated upon overexpression, we compared the aggregation kinetics of unmodified and modified α-synuclein. Whereas unmodified α-synuclein formed fibrils, modified α-synuclein remained soluble. The presence of as little as 10% sumoylated α-synuclein was sufficient to delay aggregation significantly in vitro. We mapped SUMO acceptor sites in α-synuclein and showed that simultaneous mutation of lysines 96 and 102 to arginine significantly impaired α-synuclein sumoylation in vitro and in cells. Importantly, this double mutant showed increased propensity for aggregation and cytotoxicity in a cell-based assay and increased cytotoxicity in dopaminergic neurons of the substantia nigra in vivo. These findings strongly support the model that sumoylation promotes protein solubility and suggest that defects in sumoylation may contribute to aggregation-induced diseases.

Introduction

Three different small ubiquitin-related modifier (SUMO) proteins, SUMO1 and the twins SUMO2/3, can be conjugated to their target proteins in an enzymatic pathway that resembles ubiquitination. This posttranslational modification of proteins with SUMO (sumoylation) is involved in a variety of different cellular pathways, often by regulating protein–protein or protein–DNA interactions (Johnson, 2004; Hay, 2005; Geiss-Friedlander and Melchior, 2007; Wilkinson and Henley, 2010). More recently, increasing evidence suggests that SUMO may also contribute to protein solubility (Palacios et al., 2005; Fei et al., 2006; Mukherjee et al., 2009; Janer et al., 2010).

A common feature of sporadic forms of neurodegenerative disease is a decreased solubility of specific disease-associated proteins and, concomitantly, an enhanced pathological propensity to form aggregates. The identification of point mutations, deletions, or trinucleotide extensions in aggregating proteins causing hereditary forms of neurodegenerative diseases further

Correspondence to Jochen H. Weishaupt: jweisha@gwdg.de; or Frauke Melchior: f.melchior@zmbh.uni-heidelberg.de

E. Meulmeester's present address is Leiden University Medical Center, 2300 RC Leiden, Netherlands.

G. Bossis's present address is Institut de Génétique Moléculaire de Montpellier, Centre National de la Recherche Scientifique, 34293 Montpellier, France.

Abbreviations used in this paper: LC, liquid chromatography; MS, mass spectrometry; NAC, nonamyloid component; NeuN, neuronal nuclei; NTA, nitrilotriacetic acid; PD, Parkinson's disease; SN, substantia nigra; SNpc, SN pars compacta; SUMO, small ubiquitin-related modifier; TBL, total brain lysate; TEM, transmission EM; ThioT, Thioflavin T; VMAT, vesicular monoamine transporter; WT, wild type.

The Rockefeller University Press $30.00
J. Cell Biol. Vol. 194 No. 1 49–60
www.jcb.org/cgi/doi/10.1083/jcb.201010117

JCB 49

THE JOURNAL OF CELL BIOLOGY

supports the causal role of insoluble and aggregated proteins. Pathological protein aggregation is thus a prominent feature of neurodegenerative diseases like Parkinson's disease (PD).

Several aggregation-prone proteins implicated in neurodegeneration were found to be sumoylated, and sumoylation-deficient mutants showed an enhanced tendency to aggregate in cell-based assays. Together with the observation that SUMO proteins are among the most soluble proteins known and that SUMO as an artificial fusion tag helps to produce soluble recombinant proteins (Marblestone et al., 2006; Panavas et al., 2009), it is plausible to speculate that sumoylation serves to regulate the solubility of aggregation-prone proteins.

Previous findings were based on cell-based assays only (Steffan et al., 2004; Mukherjee et al., 2009; Janer et al., 2010); therefore, we aimed to approach this hypothesis directly by measuring the aggregation propensity of a purified sumoylated and unmodified protein, namely α-synuclein, a prototypic aggregation-prone protein that can be recombinantly expressed at high levels and that plays a pivotal role in the pathogenesis of neurodegenerative diseases collectively called synucleinopathies.

α-Synuclein is a natively unfolded neuronal protein that is enriched in presynaptic terminals (Iwai et al., 1995). Although α-synuclein has been implicated in synaptic vesicle trafficking, its physiological functions remain largely enigmatic (Chandra et al., 2004, 2005). However, a central role in the pathology of PD, as well as Lewy body disease and multiple system atrophy, has been ascribed to α-synuclein. Missense mutations and increased gene dosage of α-synuclein cause autosomal-dominant PD (Polymeropoulos et al., 1997; Krüger et al., 1998; Singleton et al., 2003; Zarranz et al., 2004). Another aspect of α-synuclein is that it is a major constituent of the neuronal intracellular Lewy bodies that are a histological hallmark of PD and Lewy body disease.

Posttranslational modifications including ubiquitination, phosphorylation, and nitrosylation of α-synuclein have been reported to play a role in α-synuclein toxicity (Giasson et al., 2000; Shimura et al., 2001; Fujiwara et al., 2002). More recently, α-synuclein was found to be sumoylated upon overexpression in HEK293 cells. Based on mutagenesis/transfection experiments, lysine 102 serves as one SUMO acceptor site; however, the K102R mutant protein was still efficiently modified. To date, a function for α-synuclein sumoylation has not been published (Dorval and Fraser, 2006).

Here, we provide comprehensive and direct support for a role of sumoylation in protein aggregation in vitro and in vivo. Moreover, we show that sumoylation deficiency potentiates α-synuclein neurotoxicity.

Results

As outlined in the previous section, the prototypic aggregation-prone α-synuclein seemed like an ideal candidate to study a possible impact of sumoylation on protein aggregation in vitro and in cells. However, sumoylation of α-synuclein had so far only been observed upon overexpression in HEK293 cells (Dorval and Fraser, 2006).

α-Synuclein is sumoylated in vitro and in cell lines

We first tested whether α-synuclein can be conjugated in a cell-free system. To this purpose, recombinant α-synuclein was incubated with SUMO2, the E1-activating enzyme Aos1/Uba2, the E2-conjugating enzyme (Ubc9), and the E3 ligase PIASxα or catalytic fragments of the E3 ligase RanBP2 (BP2ΔFG and Ir1+M). As shown in Fig. 1 A (myc–α-synuclein staining), α-synuclein could be efficiently sumoylated in the presence of an E3 ligase (see Fig. S1 B for additional SUMO1 staining). Next, we confirmed α-synuclein as a target for SUMO conjugation in HEK293T cells (Fig. 1 B). Plasmids encoding His_6-tagged SUMO2 and α-synuclein were cotransfected in HEK293T cells. His_6-SUMO2 substrates were isolated by Ni^{2+} affinity chromatography. Only in the presence of His_6-SUMO2 and α-synuclein could higher molecular mass species (∼35 kD) immunopositive for α-synuclein be detected, demonstrating a covalent SUMO conjugation to α-synuclein.

### α-Synuclein is sumoylated in the brain of His_6-SUMO2 transgenic mice

To provide proof for α-synuclein sumoylation under in vivo circumstances in the brain, we generated transgenic mice expressing His_6-SUMO2 under control of the neuron-specific Thy1.2 promoter (Fig. 1 C). These animals are fertile and have no obvious abnormalities. Brain lysates from wild-type (WT) and His_6-SUMO transgenic mice were subjected to Ni^{2+} affinity chromatography to examine α-synuclein sumoylation.

In these His_6-SUMO2 transgenic mice, we observed an ∼35-kD α-synuclein immunoreactive species, which was similar to our in vitro and cellular assays, indicating that endogenous α-synuclein is sumoylated under physiological circumstances (Fig. 1 C). The specificity of the His-SUMO2 pull-down, analyzed by anti-SUMO2 immunoblotting, is shown in Fig. S1 C. Our results show that endogenous α-synuclein is efficiently conjugated with SUMO2 in the mouse brain and that our transgenic mice are suitable tools for in vivo confirmation of neuronal SUMO targets.

Sumoylation of α-synuclein abolishes amyloid fibril formation in vitro

The central disease-associated propensity of α-synuclein to aggregate in vivo can be recapitulated in vitro, as recombinant monomeric α-synuclein forms amyloid fibrils that are similar to α-synuclein filaments isolated from patients with synucleinopathies (Crowther et al., 2000; Serpell et al., 2000). Considering the high solubility of SUMO, we hypothesized that sumoylation may act as a modulator of fibril/aggregate formation, thus maintaining the aggregation-prone α-synuclein in solution. Therefore, we aimed to characterize the impact of sumoylation on α-synuclein fibril formation under in vitro conditions. As this required several milligrams of purified untagged sumoylated α-synuclein, we used a system for overproduction of sumoylated substrates in *Escherichia coli* (Uchimura et al., 2004) and purified recombinant sumoylated α-synuclein from heat-treated bacterial lysates by ion exchange chromatography and gel filtration. The aggregation propensity of sumoylated α-synuclein

A

B

C
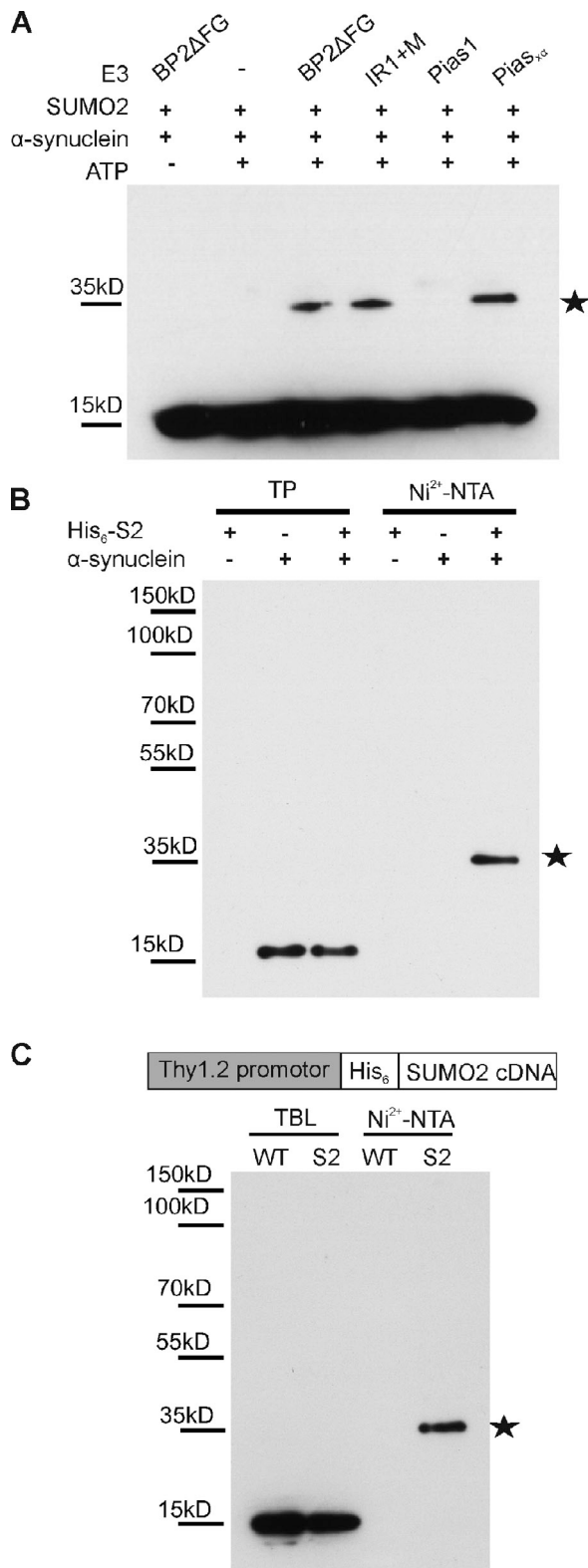
Figure 1. **α-Synuclein sumoylation in vitro in cells and in mouse brain.** (A) α-Synuclein is SUMO2 modified in vitro. 500 ng α-synuclein, 500 ng SUMO2, 150 ng Aos1/Uba2, 200 ng Ubc9, and 5–10 ng E3 ligase fragments were incubated for 30 min at 30°C with and without ATP in a volume of 20 µl. Reactions were stopped with SDS sample buffer before analysis by SDS-PAGE and immunoblotting with mouse monoclonal anti–α-synuclein antibody (Syn211; Invitrogen). (B) α-Synuclein modification by SUMO2 in HEK293T cells. Plasmids encoding His$_6$-SUMO2 (His$_6$-S2) or/and α-synuclein were transfected in HEK293T cells. SUMO substrates were purified by

was then compared with that of unconjugated α-synuclein purified under the same conditions (Fig. 2). The in vitro fibrillation process was monitored via Thioflavin T (ThioT) fluorescence. Interestingly, sumoylation of α-synuclein completely abolished fibril formation even after 146 h of incubation (Fig. 2, A–C). In contrast, the presence of equimolar amounts of nonconjugated SUMO did not prevent fibril formation (Fig. 2, A, B, and D). Transmission EM (TEM) images confirmed the absence of fibril formation in the sumoylated α-synuclein sample (Fig. 2 C) and the presence of amyloid fibrils formed by untagged recombinant α-synuclein in a mixture with nonconjugated SUMO (Fig. 2 D).

In intact cells, only a small fraction of specific targets is usually sumoylated at a steady state. This can be a result of rapid cycles of conjugation and deconjugation or temporal or local control of sumoylation. Low levels of sumoylation are also observed for α-synuclein, as shown in Fig. 1 B for transfected cell cultures and in Fig. 1 C for brain from transgenic SUMO2 mice. Therefore, it was important to test whether α-synuclein fibrillation would also be affected when <100% α-synuclein was modified. Therefore, we mixed modified and unmodified α-synuclein at ratios of 1:1 and 1:9 and again analyzed fibril formation. As shown in Fig. 2 (F and G), 50% of sumoylation was sufficient to completely block α-synuclein fibrillation in vitro (Fig. 2, E–G). Most remarkable, however, was that α-synuclein sumoylated to 10% was sufficient to cause an impressive 60-h delay in fibril formation (Fig. 2, I and J). After 110 h of incubation, the fibrillation of α-synuclein sumoylated to 10% reached a steady state. Of note, the addition of free SUMO in concentrations corresponding to 10, 50, or 100% unmodified α-synuclein had no effect on α-synuclein fibrillation (Fig. 2, D, H, and L). Our results illustrate that sumoylated α-synuclein fails to form fibrillar aggregates and that the covalent conjugation of a single SUMO molecule even to a small proportion of α-synuclein molecules substantially delays its fibril formation.

α-Synuclein has multiple SUMO acceptor sites, the most significant of which are lysines 96 and 102

To test whether sumoylation also contributes to α-synuclein solubility in cells, we needed to identify a sumoylation-deficient mutant. Although sumoylation of α-synuclein on lysine 102 had been previously described (Dorval and Fraser, 2006), residual sumoylation suggests that additional lysines are also subjected to sumoylation. We thus mapped α-synuclein SUMO acceptor sites by a combination of mutagenesis and mass spectrometry

Ni^{2+} affinity chromatography (Ni^{2+}-NTA) under denaturing conditions, and a sumoylated α-synuclein band at ∼35 kD (stars in A and B) was detected with an α-synuclein antibody (Syn211). 1% of total input (TP) and 25% of elution fractions were loaded. (C, top) A schematic representation of the Thy1.2/His$_6$-SUMO transgene. (bottom) α-Synuclein sumoylation in mouse brain tissue. Total His$_6$-SUMO2–conjugated proteins were isolated using Ni^{2+}-NTA affinity chromatography. TBLs and eluates were probed with anti–α-synuclein antibody recognizing mouse α-synuclein (clone 42). α-Synuclein modified by a single SUMO2 molecule, indicated with a star, could be detected in the eluate obtained from His$_6$-SUMO2 transgenics.
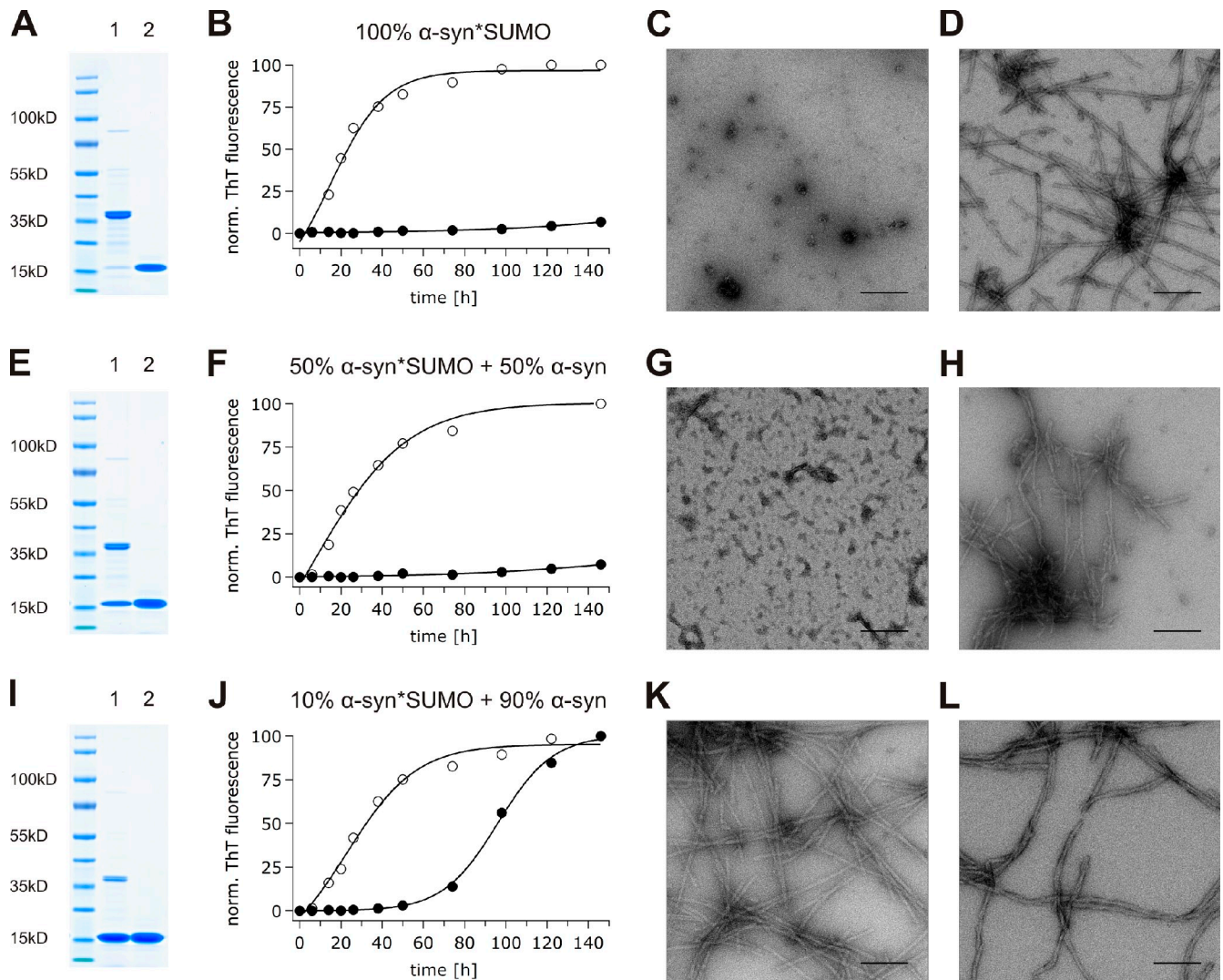
Figure 2. **In vitro fibril formation of sumoylated α-synuclein.** (A) Coomassie staining of α-synuclein sumoylated to 100% (lane 1) and α-synuclein with an equimolar amount of free SUMO1 (lane 2). (B) Fibrillization kinetics of α-synuclein sumoylated to 100% (70 µM; closed circles) and control condition (70 µM of nonmodified α-synuclein + 70 µM of free SUMO1; open circles). (C) Nonamyloidogenic amorphous oligomers formed by α-synuclein sumoylated to 100%. (D) Mature fibrils formed by control nonmodified α-synuclein in the presence of 70 µM of free SUMO1. (E) Coomassie staining of α-synuclein sumoylated to 50% (lane 1) and α-synuclein with an equimolar amount of free SUMO1 (lane 2). (F) Fibrillization kinetics of α-synuclein sumoylated to 50% (35 µM sumoylated α-synuclein + 35 µM of nonmodified α-synuclein; closed circles) and control condition (70 µM of nonmodified α-synuclein + 35 µM of free SUMO1; open circles). (G) Nonamyloidogenic amorphous material formed by α-synuclein sumoylated to 50%. (H) Mature fibrils formed by control nonmodified α-synuclein in the presence of 35 µM of free SUMO1. (I) Coomassie staining of α-synuclein sumoylated to 10% (lane 1) and α-synuclein with an equimolar amount of free SUMO1 (lane 2). (J) Fibrillization kinetics of α-synuclein sumoylated to 10% (7 µM sumoylated α-synuclein + 63 µM of nonmodified α-synuclein; closed circles) and control condition (70 µM of nonmodified α-synuclein + 7 µM of free SUMO1; open circles). (K) Mature fibrils formed by α-synuclein sumoylated to 10%. (L) Mature fibrils formed by control nonmodified α-synuclein in the presence of 7 µM of free SUMO1. (C, D, G, H, K, and L) TEM of aggregation samples after 146 h of incubation in 50 mM Hepes and 100 mM NaCl, pH 7.4, at 37°C with constant stirring. ThT, Thioflavin T. Bars, 200 nm.

(MS) approaches (Hsiao et al., 2009). α-Synuclein contains one classical SUMO consensus acceptor site (K96: VKxD) and another closely related motif (K102: GKxE). Hence, we generated single point mutations replacing K96 or K102 by an arginine. In addition, we constructed double and triple lysine-to-arginine mutants mR1 (K6R, K10R, and K12R), mR2 (K21R and K23R), mR3 (K32R and K34R), mR4 (K43R and K45R), or mR5 (K58R and K60R) for the remaining nonconsensus lysines. However, none of these α-synuclein mutations completely abolished or substantially reduced SUMO conjugation in HEK293T cells (Fig. 3 A). We then turned to the bacterially produced sumoylated

α-synuclein and identified modified lysine residues by MS analysis (Hsiao et al., 2009). Of note, although we were able to record and annotate fragment spectra (tandem MS [MS/MS]), proving that K96 is indeed sumoylated (Fig. S2 A), we could not obtain a similar spectrum for a tryptic peptide derived from sumoylated α-synuclein with SUMO conjugated to K102. In this case, we only recorded the exact molecular weight of this particular peptide (Fig. S2 B). Recording and annotation of a fragment spectrum of this particular peptide were hampered by the fact that the peptide (a) is very big (>6,900 D); (b) shows a charge state of +5 of the intact mass and, consequently upon fragmentation,
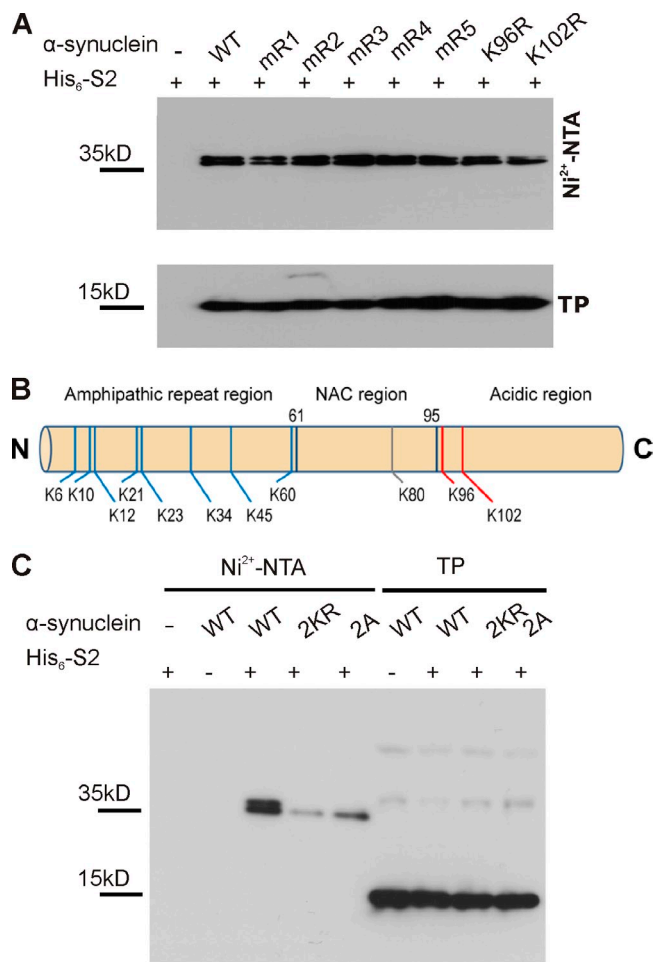
Figure 3. **K96 and K102 are the major sumoylation sites of α-synuclein.**
(A) α-Synuclein is sumoylated at multiple lysine residues. Sumoylation of α-synuclein was analyzed in HEK293T cells by cotransfection of His_6-SUMO2 with WT myc-tagged α-synuclein or one of the indicated lysine-to-arginine mutants (mR1: K6, 10, and 12R; mR2: K21 and 23R; mR3: K32 and 34R; mR4: K43 and 45R; and mR5: K58, 60R, K96R, and K102R), followed by Ni^{2+}-NTA chromatography. None of the mutations resulted in abolished α-synuclein sumoylation. Total protein (TP) levels of WT α-synuclein and the respective mutants are shown in the bottom panel. Samples were analyzed by immunoblotting with anti-myc antibody (9E10). (B) Summary of α-synuclein sumoylation sites. MS analysis of sumoylated α-synuclein (obtained upon sumoylation in bacteria; see Materials and methods) revealed 11 SUMO-conjugated lysine residues (8 lysines in the N-terminal amphipathic region, 1 lysine in the hydrophobic NAC region, and the 2 lysines in the C-terminal acidic region; Fig. S2 and supplemental data). Nonconsensus lysines are depicted in blue, and the consensus and consensus sequence–related sites are in red. (C) The sumoylation levels of myc-tagged WT, 2KR (K96R and K102R), and 2A (D98A and E104A) mutants were compared using Ni^{2+}-NTA chromatography. Elution samples and total lysates (TP) in A and C were run on a 4–12% NuPAGE Bis-Tris gel and analyzed by immunoblotting with myc antibody (clone 9E10). Sumoylated α-synuclein runs as a doublet band on gradient SDS-PAGE.

the charge states +4, +3, +2, and +1, which complicates the annotation and sequence assignment; and, (c) most importantly, that this particular peptide encompasses the extreme C terminus of α-synuclein that lacks a C-terminal lysine or arginine and is thus not favorable for fragmentation under our conditions per se. In total, the size of the peptide together with its nontryptic nature prevented the generation of a meaningful fragment spectrum. Nonetheless, the exact mass of this particular peptide as revealed

in the Orbitrap mass analyzed (Fig. S2 B) strongly suggests that this peptide is indeed the C terminus of α-synuclein sumoylated at K102. No other tryptic fragment derived from α-synuclein with or without conjugation with SUMO reveals a similar intact mass. We could thereby confirm K96 and K102 in the acidic C-terminal region as SUMO acceptor sites and, in addition, found eight other lysines in the N-terminal amphipathic region as well as the single lysine (K80) in the nonamyloid component (NAC) region (Figs. 3 B and S2 and supplemental data). In conclusion, at least 11 out of its 15 lysine residues can serve as SUMO acceptor sites. This is in line with our observation that, based on the migration behavior in polyacrylamide gels and despite the fact that α-synuclein is predominantly mono-sumoylated, we sometimes observed faint, higher migrating additional bands that probably correspond to a minor proportion of polysumoylated α-synuclein. However, two lysine residues in close proximity to each other (K96 and K102) account for >50% of the α-synuclein SUMO conjugates, as simultaneous mutation of both lysines (2KR double mutant) strongly impaired sumoylation (Fig. 3 C). This double mutant served in the following cell-based analysis as a sumoylation-deficient mutant. However, because mutation of lysine residues may also influence ubiquitination or acetylation, we wanted to have one additional mutant for functional assays. Therefore, we tested whether mutagenesis of the two acidic residues adjacent to the SUMO acceptor lysines would also affect sumoylation (consensus SUMO acceptor sites require the acidic residue; Sapetschnig et al., 2002). Indeed, mutation of D98A and E104A (2A mutant) impairs sumoylation to a similar extent as the lysine-to-arginine mutations (Fig. 3 C). Of note, the ubiquitination status of α-synuclein was not altered by mutating K96 and K102 (Fig. S3).

Impaired sumoylation of α-synuclein increases inclusion formation and toxicity in HEK293T cells

Having identified two different α-synuclein variants that are impaired in sumoylation, we wanted to compare their aggregation propensity and cytotoxicity with WT α-synuclein. For this, we used a technique that allows visualization of α-synuclein inclusion formation in HEK293T cells (Opazo et al., 2008) by indirect GFP labeling. Using this method, we transfected cells either with WT α-synuclein or the mutants in which the main SUMO acceptor sites were abolished (2KR and 2A), all fused to a short (six amino acids) PDZ binding tag. WT α-synuclein and mutant variants were coexpressed with a PDZ domain–GFP fusion protein. This approach allows GFP labeling of α-synuclein by binding of the PDZ domain–GFP fusion protein to the small PDZ binding tag of α-synuclein after both proteins have been expressed in cells. The technique avoids the use of an α-synuclein–GFP fusion protein, which bears a risk of altering α-synuclein characteristics, including aggregation and toxicity, compared with the untagged protein (see Materials and methods; Opazo et al., 2008).

Cells were fixed 36 h after transfection, and the GFP fluorescence distribution pattern was quantified in a blinded fashion as follows: cells with homogenous α-synuclein distribution (Fig. 4 A), cells with aggregates (Fig. 4 B), or cells with fragmented

Homogenous	Inclusions	Apoptotic
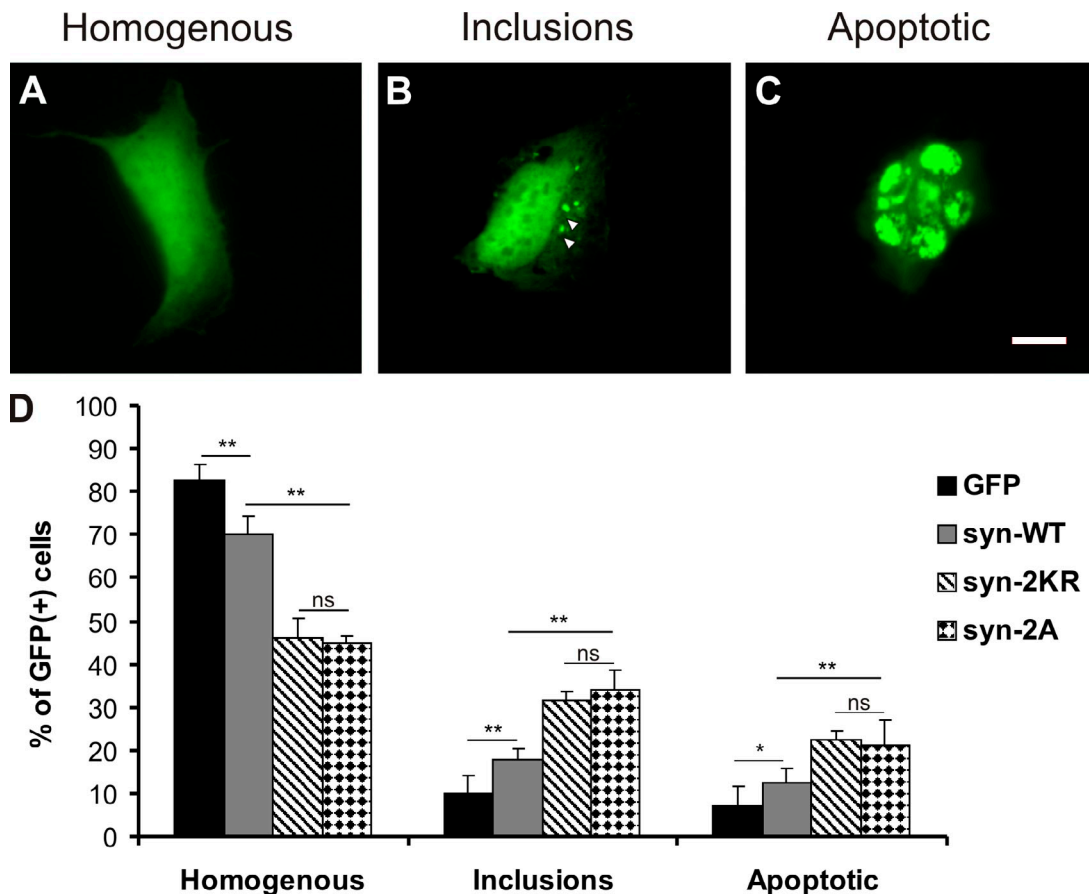
Figure 4. **Sumoylation-impaired α-synuclein mutants (2KR and 2A) induce increased toxicity and inclusion formation compared with WT α-synuclein in HEK cells.** (A–D) HEK293T cells were transfected with bicistronic plasmids expressing α-synuclein variants (syn-WT; 2KR: K96 and 102R; and 2A: D98A and E104A) with a PDZ binding tag (HSTTRV) and PDZ domain–EGFP fusion protein (GFP). (A–C) Cells were classified in three groups based on GFP fluorescence distribution: homogenous (A), containing intracellular GFP-positive inclusions (B, arrowheads), and preapoptotic or having fragmented nuclei by DAPI staining (C). Images display exemplary cells to illustrate the different categories into which cells were grouped. Because individual cells displayed variations in expression levels, exposure times were adjusted differently to avoid overexposure. At the level of total cell lysates, expression levels of the different constructs were the same between the different experimental conditions. Bar, 20 µm. (D) Bar graphs represent percentages of all GFP-positive cells in the three categories summarized as mean ± SEM. Comparisons were made with KyPlot 5.0 using Student's *t* test (*, $P < 0.05$; **, $P < 0.01$). $n = 6$. Note that cell counts were performed by direct observation at the microscope using identical optical parameters for all experimental conditions. ns, not significant.

nuclei, the latter being indicative of cytotoxicity and apoptosis (Fig. 4 C). In agreement with our in vitro fibrillation assay, we observed that α-synuclein that is largely sumoylation resistant (2KR mutant) leads to an increased proportion of cells with α-synuclein inclusions/aggregates (Fig. 4 D). Moreover, the α-synuclein–2KR mutant was substantially more toxic than WT α-synuclein as measured by an increased apoptosis rate (Fig. 4 D). Importantly, the α-synuclein 2A mutant (2A: D98A and E104A) that has no lysine substitutions behaved like the 2KR variant, which further corroborates the hypothesis that the altered aggregation properties and enhanced neurotoxicity indeed represent sumoylation-dependent effects.

Mutations in the major SUMO acceptor sites of α-synuclein exacerbate toxicity in dopaminergic neurons in vivo

Thus far, our results showed that covalent conjugation of a single SUMO molecule to α-synuclein prevents it from fibril formation in vitro and provides evidence that sumoylation of α-synuclein reduces both its aggregation and toxicity in HEK293T cells. To address specifically the role that SUMO plays in the regulation of α-synuclein–induced toxicity in dopaminergic neurons in vivo, we compared the toxicity of WT α-synuclein with α-synuclein–2KR in a rat model of PD. To this end, we expressed α-synuclein in dopaminergic substantia nigra (SN) neurons by recombinant adeno-associated viral vector serotype 2 (rAAV2)–mediated gene transfer. Overexpression of α-synuclein in dopaminergic neurons is a valid in vivo model for PD. It finds its equivalent in an enhanced expression as a result of α-synuclein gene duplications or triplications, which cause familial forms of PD (Singleton et al., 2003; Miller et al., 2004).

rAAV2 expressing EGFP, WT α-synuclein, or α-synuclein–2KR under a neuron-specific promoter (Fig. 5 A) were stereotactically injected into the left SN pars compacta (SNpc) of female Wistar rats. Brainstem sections were double stained for the dopaminergic cell marker vesicular monoamine transporter 2 (VMAT2) and human α-synuclein 12 wk after injection.
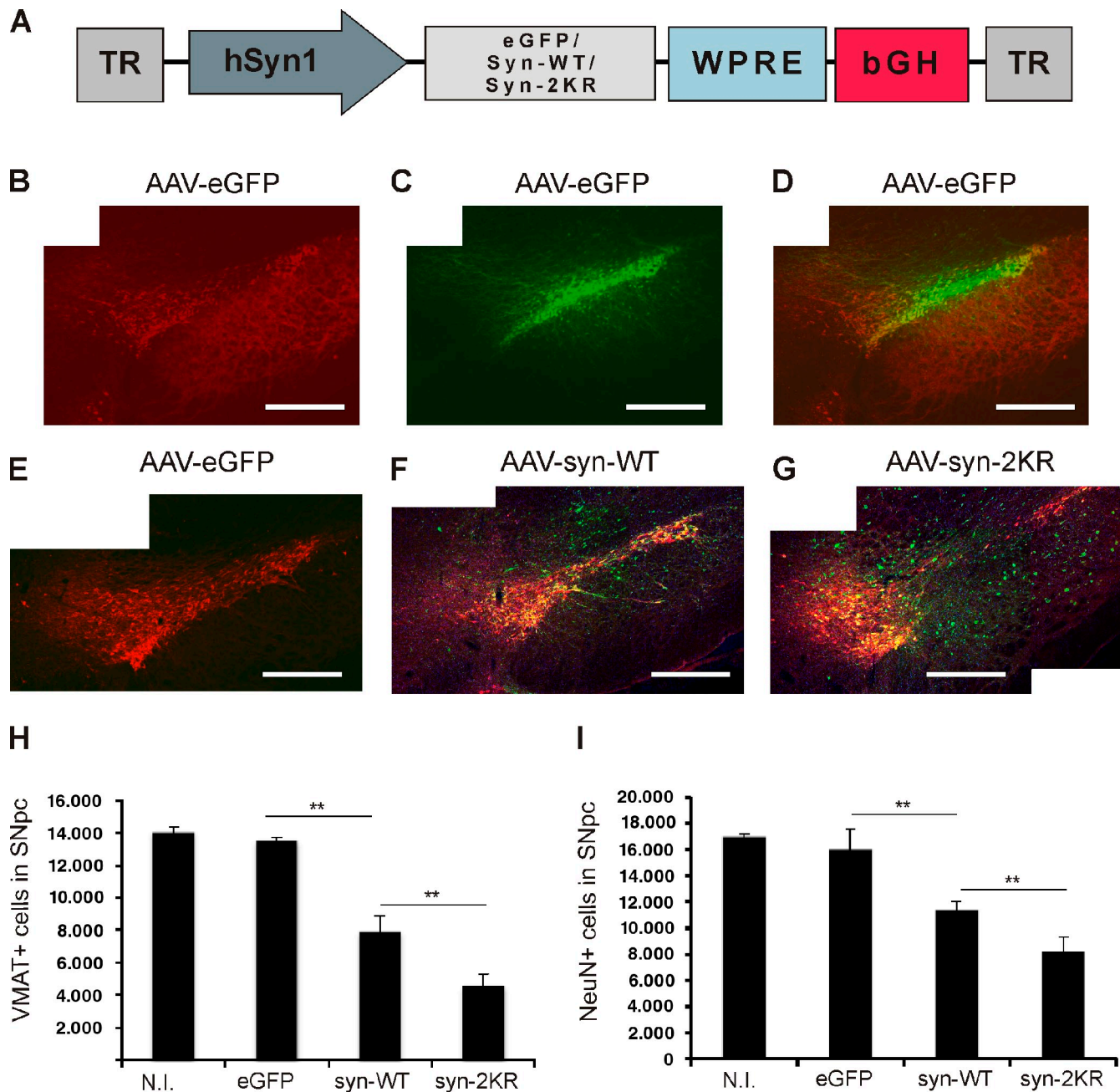
Figure 5. **Reduced sumoylation exacerbates α-synuclein neurotoxicity in vivo.** (A) A schematic representation of vector genomes used in the in vivo rat model of PD. Recombinant adeno-associated viral vectors (AAV2) express either EGFP, WT α-synuclein (syn-WT), or α-synuclein K96R and K102R (syn-2KR) under the control of neuron-specific human synapsin 1 gene promoter (hSyn1). Vectors also encode inverted terminal repeats (TR) and small control elements woodchuck hepatitis virus posttranscriptional control element (WPRE) and bovine growth hormone (bGH)–derived polyadenylation site. (B) VMAT2-positive (VMAT2+) neurons (red) in the left SN. (C) rAAV2-mediated GFP transduction of SNpc. (D) Overlay of VMAT2+ and GFP-transduced neurons in the left SN. (E–G) Coimmunostaining of VMAT2+ (red) and human α-synuclein (green). Survival of VMAT2+ neurons in SNpc of animals injected with rAAV2 vectors expressing EGFP (E), human WT α-synuclein (F), or α-synuclein–2KR (G). Panels B–G are each a composite of two separate fluorescent images (Axioplan2 with a 5× objective and AxioVision 4.7). (H and I) Respective unbiased stereological quantification of surviving VMAT2+ (H) or NeuN+ (I) cells in the transduced SNpc. The graphs display VMAT2+ or NeuN+ cell numbers in animals injected with rAAV2 expressing EGFP, WT α-synuclein (syn-WT), and α-synuclein–2KR (syn-2KR). N.I., contralateral noninjected side. n = 6–8 per experimental group. Results are mean ± SEM. **, P < 0.01, Student's t test. Bars, 0.5 mm.

Proper neuronal transgene targeting is shown by fluorescence of EGFP and overlapping immunoreactivity for human α-synuclein in VMAT2+ SNpc cells (Fig. 5, A–C). Transgene expression levels were assessed in cultured primary rat cortical neurons (Fig. S4). Blind quantification of dopaminergic (VMAT2+) SNpc neurons was performed by a stereological technique. Quantification revealed that injection of EGFP in the SNpc did not affect the survival of dopaminergic (VMAT2+) neurons compared with the noninjected contralateral SNpc. However, injection of WT α-synuclein resulted in a significant loss of VMAT2+ SNpc neurons (7,897 ± 1,007 surviving VMAT2+ cells in WT α-synuclein compared with 13,505 ± 201 in the EGFP control; P < 0.01;

Fig. 5, E and G), recapitulating the effect of increased gene dosage and overexpression of α-synuclein in hereditary forms of PD (Singleton et al., 2003; Miller et al., 2004). Injection of rAAV2 encoding α-synuclein that is largely impaired in sumoylation (synuclein-2KR) substantially exacerbated this neurodegenerative effect (4,577 ± 704 surviving dopaminergic SNpc neurons or 42% less survival compared with WT α-synuclein; P < 0.01; Fig. 5, F and G).

We then confirmed our results by an additional stereological evaluation using neuronal nuclei (NeuN) as a neuronal marker independent of the dopaminergic phenotype. As expected, we observed overall higher absolute cell numbers in all groups compared with the dopamingergic cell marker VMAT2 (Fig. 5 H). Importantly, both the toxic effect of WT α-synuclein and exacerbated toxicity of the sumoylation-deficient mutant could be recapitulated after evaluating the surviving NeuN-positive neurons (Fig. 5 I). This result suggests that endogenous sumoylation of α-synuclein at the main K96/K102 SUMO acceptor sites greatly reduces its neurotoxicity on dopaminergic SNpc neurons in vivo.

Discussion

In this study, we provide direct in vitro and in vivo evidence for SUMO's contribution to keeping an aggregation-prone protein soluble. We characterize sumoylation of α-synuclein as a prototypic aggregating disease protein, show that sumoylation of α-synuclein inhibits its fibrillation, and show that mutation of the main α-synuclein SUMO acceptor sites leads to increased toxicity.

SUMO modification maintains soluble α-synuclein

Because SUMO is one of the most soluble proteins (Bayer et al., 1998) whose attachment as an artificial fusion tag helps to produce otherwise difficult-to-purify proteins (Marblestone et al., 2006; Panavas et al., 2009), we examined whether the physiologically occurring modification of the aggregation-prone α-synuclein by SUMO prevents its fibrillation. To that end, we generated large quantities of both sumoylated and nonmodified recombinant α-synuclein. We did indeed observe that SUMO modification of α-synuclein abolishes its fibril formation. This is the first time that SUMO's impact on protein solubility and aggregation could be demonstrated directly in cell-free in vitro conditions. In agreement, we observed an increased aggregate formation in cells when the two major SUMO modification sites in α-synuclein were abolished.

Both in cell-free assays and in cell culture, only a small fraction of α-synuclein was sumoylated. However, this does not challenge the functional relevance of our finding. Low steady-state levels of the highly dynamic SUMO modification can have a major impact on a specific protein's function (Hardeland et al., 2002; Baba et al., 2005). Even if only a small percentage of α-synuclein is modified at a steady state, the entire pool can go through rapid rounds of sumoylation and desumoylation, and, thus, the modification can have a significant impact on the formation or resolution of α-synuclein inclusions. Importantly, we

found that 50% α-synuclein sumoylation was sufficient to completely abolish β-sheet/fibril formation in vitro and that as little as 10% sumoylation substantially delayed fibril formation.

Steric hindrance of α-synuclein fibrillation by SUMO?

The exact molecular mechanism that leads to inhibition or delay in fibril formation upon sumoylation of α-synuclein remains unknown; however, a possible explanation is as follows: PD-associated amyloid fibrils are formed from protofibrils, which is characteristic for β-sheet structures. Biochemical analysis and solid-state nuclear magnetic resonance experiments have revealed a 7-kD fragment of α-synuclein, comprising residues 31–109, as a proteinase K–resistant core of the amyloid fibril (Miake et al., 2002; Heise et al., 2005; Vilar et al., 2008). Moreover, the C terminus of α-synuclein is negatively charged, and there is evidence to suggest that its interaction with the NAC domain inhibits the aggregation of α-synuclein (Bertoncini et al., 2005). The two main SUMO acceptor sites K96/K102 that we identified are thus in very close proximity to the aggregation-promoting amino acid stretch. Therefore, the steric barrier and shielding of the aggregation-promoting hydrophobic core may account for impaired fibril formation of sumoylated α-synuclein. A similar inhibitory effect on in vitro α-synuclein fibril formation has been observed by the addition of Hsp70 to the aggregation sample (Dedmon et al., 2005), which is probably a result of its binding to the hydrophobic core of α-synuclein or to prefibrillar intermediates. Nuclear magnetic resonance studies are planned to pursue this hypothesis at a structural level.

SUMO as a general solubility enhancer?

Our findings also raise the interesting possibility that dynamic conjugation and deconjugation of the highly soluble SUMO to several varying lysine residues throughout the protein may fulfill chaperone-like functions and keep the highly aggregation-prone α-synuclein fractions in solution. This would be in agreement with the presence of multiple alternative sumoylation sites in α-synuclein, suggesting that the aggregation-inhibiting effect of SUMO modification may not be site specific. Similarly, a linear SUMO-huntingtin fusion protein displayed enhanced solubility (Steffan et al., 2004) independently from the SUMO acceptor site. Moreover, sumoylation has been suggested to modulate the solubility of aggregopathy-related proteins like superoxide dismutase-1 and proteins with CAG repeat expansion (Fei et al., 2006; Mukherjee et al., 2009; Janer et al., 2010). Altogether, we therefore see the emerging general concept that sumoylation keeps α-synuclein and other aggregation-prone proteins in solution.

Sumoylation: possible relevance for neurodegeneration

Fibril and aggregate formation are suspected to be important contributors to α-synuclein neurotoxicity (Duda et al., 2000; Irvine et al., 2008). In our work, we identified a sumoylation-deficient α-synuclein mutant (2KR) with an enhanced propensity to aggregate. It displayed substantially increased toxicity in a cell line as well as in the rAAV rat model of PD. Similarly, the solubility of the aggregation-prone ataxin 7 and androgen receptor
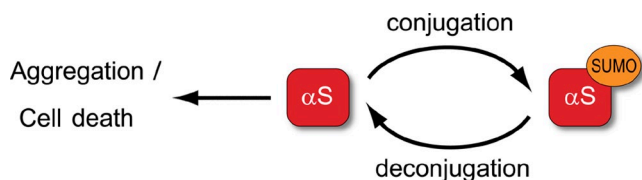
Figure 6. Proposed model for the role of sumoylation in α-synuclein–induced neurodegeneration. SUMO prevents aggregation-prone fractions of α-synuclein (αS) from fibril formation. Impaired sumoylation may enhance the formation of α-synuclein toxic species, which results in aggravated dopaminergic cell death.

with triplet repeat expansion was enhanced upon sumoylation and resulted in less toxicity (Mukherjee et al., 2009; Janer et al., 2010). Although these data implicate a beneficial effect of α-synuclein sumoylation on neuronal cell survival, reduction of the SUMO levels improved neuropathology in another in vivo neurodegeneration paradigm, the *Drosophila melanogaster* model of Huntington's disease (Steffan et al., 2004). However, in this case, enhanced toxicity, despite reduced aggregate formation, was accompanied by a stronger capacity to repress transcription in an in vitro assay. Hence, sumoylation of neurodegeneration-inducing substrates can alter their deleterious effect in either way, intensifying or reducing it, which is in agreement with the generally highly target-specific cell biological effects of SUMO modification.

Thus, it is tempting to speculate that modification with SUMO proteins may play a role in the pathophysiology of PD; in addition to possible—so far, unknown—genetic defects that may alter the equilibrium of reversible sumoylation, the SUMO pathway is known to respond dramatically to many different insults and environmental stresses, including heat, oxidative stress, viral and bacterial infection, and ischemia (Bossis and Melchior, 2006; Kindsmüller et al., 2007; Cimarosti and Henley, 2008; Cimarosti et al., 2008; Yang et al., 2008; Chang et al., 2009). Specifically, oxidative stress has been linked to PD. For example, an increase in production of reactive oxygen species as a result of mitochondrial dysfunction has been observed in animal models and implicated in the pathogenesis of PD (Fukae et al., 2007; Zhou et al., 2008).

In conclusion, we provide a comprehensive in vitro and in vivo analysis that reveals SUMO's impact on protein aggregation properties using a prototypic disease-related protein prone to forming pathological intracellular inclusion bodies. Impaired sumoylation of overexpressed α-synuclein contributes to PD-related characteristics of α-synuclein, neurotoxicity, and fibril formation (Fig. 6). To determine whether genetic, environmental, or oxidative stress–induced changes in sumoylation contribute to the disease development will require extensive future investigations.

Materials and methods

In vitro sumoylation
In vitro sumoylation assays were performed in a total volume of 20 µl in SUMO assay buffer (110 mM KOAc, 20 mM Hepes, pH 7.3, 2 mM Mg[OAc]$_2$, 1 mM EGTA, 1 mM DTT, 0.2 mg/ml BSA, and 0.05% Tween 20) supplemented with protease inhibitors (Werner et al., 2009). The reactions contained 0.5 µg recombinant SUMO2, 0.5 µg recombinant α-synuclein, and

recombinant enzymes E1 (150 ng), E2 (200 ng), and E3 ligase (5–10 ng). Reactions, excluding controls, were incubated with 1 mM ATP at 30°C for 30 min, stopped by addition of SDS sample buffer, and analyzed by SDS-PAGE and immunoblotting.

Recombinant expression and purification of sumoylated α-synuclein
For large-scale generation of sumoylated α-synuclein, we made use of a coexpression system developed by Uchimura et al. (2004). For this, the tricistronic plasmid pT-E1E2S1 (provided by H. Saitoh, Kumamoto University, Kumamoto, Japan) driving overexpression of E1 and E2 enzymes and SUMO1 was cotransformed with nontagged human WT α-synuclein in pT7-7 vector in BL21 (DE3) cells. Recombinant protein expression was induced at OD$_{600}$ 0.5–0.6 with 0.5 mM IPTG, and cells were grown overnight at 30°C. Cells were harvested and resuspended in 10 mM Tris, pH 8.0, and 1 mM EDTA, pH 8.0, and lysed using an emulsion flex (EmulsiFlex-C3; Avestin). After 20 min of boiling at 95°C and 100,000-g centrifugation, the supernatant was subjected to streptomycin sulfate at 10 mg/ml to precipitate DNA. After centrifugation at 100,000 g, the supernatant was precipitated using ammonium sulfate (to 0.36 g/ml). After centrifugation, the pellet was resuspended in 25 mM Tris-HCl, pH 7.7, and loaded onto a MonoQ column (GE Healthcare). Fractions containing sumoylated α-synuclein (α-synuclein*SUMO) were pooled, desalted on a PD10 column, and run a second time on the MonoQ column. After concentration, the sample was further purified using gel filtration in 50 mM Hepes and 100 mM NaCl, pH 7.4 (Superdex S75; GE Healthcare). 10 liters of overnight culture was used for purification of 2 mg sumoylated α-synuclein. The SUMO1 isoform was used for the production of sumoylated α-synuclein in *E. coli* because SUMO2 chain formation complicated purification and drastically decreased the yield of mono-SUMO–conjugated substrate.

Ni^{2+}–nitrilotriacetic acid (NTA) affinity chromatography
His-tagged, SUMO-conjugated α-synuclein was purified from cell culture lysates or brain homogenate using Ni^{2+}-NTA affinity chromatography under denaturing conditions. Ni^{2+}-NTA affinity chromatography with cell culture lysates was performed as previously described (Jaffray and Hay, 2006). In brief, cells were lysed in 6 M guanidinium-HCl, 0.1 M Na$_2$HPO$_4$/NaH$_2$PO$_4$, and 0.01 M Tris-HCl, pH 8.0, plus 10 mM imidazole, and lysates were incubated with Ni^{2+}-NTA resin. Unbound material was washed out, and His-tagged, SUMO-conjugated proteins were eluted in 250 µl of buffer A (8 M urea, 100 mM NaH$_2$PO$_4$/Na$_2$HPO$_4$, and 10 mM Tris-HCl, pH 8.0, supplemented with 20 mM N-ethylmaleimide, 1 µg/µl aprotinin, 1 µg/µl leupeptin, and 1 µg/µl pepstatin) plus 250 mM imidazole. Pulldown experiments from mouse brain homogenates were performed as follows: 12-wk-old mice were decerebrated, and the brains were isolated and frozen in liquid nitrogen. Brain material was homogenized by grinding in liquid nitrogen and resuspended in 10 ml of buffer A. Lysates were sonicated and centrifuged for 1 h at 100,000 g and at 8°C for the removal of debris. Supernatant was recovered and incubated with 500 µl Ni^{2+}-agarose equilibrated in buffer A on a rotary shaker for 3 h at 8°C. After extensive washing with buffer A supplemented with 10 mM imidazole, buffer A supplemented with 0.2% Triton X-100 and 20 mM imidazole, buffer A supplemented with 0.1% Triton X-100 and 10 mM imidazole, and buffer A, bound proteins were eluted with 500 µl of buffer A, pH 8.0, with 250 mM imidazole. Eluates and total brain lysate (TBL) aliquots were methanol-chloroform precipitated, and protein pellets were air dried and resuspended in SDS sample buffer, separated on 4–12% NuPAGE Bis-Tris gradient gels (Invitrogen), transferred on a nitrocellulose membrane, and probed with anti–α-synuclein antibody (clone 42, 610787; BD).

Electrospray ionization–MS/MS for identification of SUMO sites
SUMO1-conjugated α-synuclein (purified as described in the Recombinant expression and purification . . . section) was excised from gel, reduced with 50 mM DTT, alkylated with 100 mM iodacedamide, and in-gel digested with modified trypsin (Promega) overnight, all at 37°C. Tryptic peptides were dissolved in 2 µl of 50% acetonitrile in 18 µl of 0.1% formic acid for further MS analysis. Mass spectrometric analysis was performed by using a linear trap quadrupole mass spectrometer (Orbitrap; Thermo Fisher Scientific) equipped with a nanoelectrospray ion source and coupled to an HPLC system (model 1100; Agilent Technologies) fitted with a homemade C18 column. Tryptic peptides were first loaded at a flow rate of 10 µl/min onto a C18 trap column, which was packed 1.5 cm in length with C18 material (Reprosil-Pur 120 Å, 5 µm, C18-AQ; Dr. Maisch GmbH) in a 360-µm outer diameter, 150-mm inner diameter capillary. Retained peptides were eluted and separated on an analytical C18 capillary column, which was packed 15 cm in length with C18 material (Reprosil-Pur 120 Å, 5 µm, C18-AQ; Dr. Maisch GmbH) in a 360-µm outer diameter,

75-mm inner diameter capillary at a flow rate of 300 nL/min, with a gradient from 7.5 to 37.5% acetonitrile in 0.1% formic acid for 60 min. Typical mass spectrometric conditions were as follows: spray voltage of 1.8 kV; heated capillary temperature of 150°C; and normalized collision-induced dissociation collision energy of 37.5% for MS/MS in linear trap quadrupole. An activation of q = 0.25 and an activation time of 30 ms were used. The mass spectrometer was operated in the data-dependent mode to automatically switch between MS and MS/MS acquisition. Full-scan survey MS spectra (from m/z = 350–2,000) were acquired in the Orbitrap with a resolution of R = 30,000 at m/z = 400 (after accumulation to a target value of 1,000,000 in the Orbitrap). The five most intense ions were sequentially isolated and fragmented in the linear ion trap using collision-induced dissociation at a target value of 100,000. For all measurements with the Orbitrap detector, a lock-mass ion from ambient air (m/z = 445.120025) was used for internal calibration.

Identification of sumoylated lysine residues was performed exactly as described in Hsiao et al. (2009). ChopNSpice software (Hsiao et al., 2009) was used to generate a concatenated protein sequence in order to identify the actual SUMO sites with the MASCOT search engine. For this, the FASTA sequence of α-synuclein was chopped into tryptic fragments allowing zero to three missed cleavages. The tryptic peptide sequence of SUMO1 that is putatively attached to any lysine residue within α-synuclein is attached to the N terminus of each tryptic peptide of α-synuclein that contains a lysine residue and a missed cleavage site. To avoid the generation of nonnatural peptides, a virtual amino acid "J" is attached to the C terminus of each tryptic fragment derived from α-synuclein and SUMO1. The thus modified tryptic fragments are concatenated to yield a large novel FASTA sequence that is submitted into database search. Upon a database search with the search engine MASCOT, cleavage with an artificial endoproteinase was allowed that specifically recognizes N- and C-terminal J and a user-defined number of missed cleavages. The search engine then compares the in silico–generated and –concatenated tryptic peptides derived from α-synuclein attached to a tryptic peptide derived from SUMO1 with the experimentally obtained fragment spectra by liquid chromatography (LC)–MS/MS (Hsiao et al., 2009). The following parameters were used in the ChopNSpice software: the spice species was *Homo sapiens*; the spice sequence was SUMO1; the spice site was KX; the spice mode was once per fragment; include unmodified fragments in output; the enzyme was trypsin; allow up to three protein miscleavages; allow up to one miscleavage in the spice sequence; the output formatting was FASTA (single protein sequence); mark all cleaved sites J; and retain comments in FASTA format without line breaks in FASTA output. For sumoylated site identification with MASCOT, all MS/MS spectra were searched against a new FASTA file that was created by ChopNSpice with the following parameters: mass tolerance of 10 ppm in MS mode and 0.8 D in MS/MS mode; allow zero missed cleavages; consider methionine oxidation and cysteine carboxyamidomethylation as variable modifications; and enzyme cleaved at J at N and C termini for MASCOT (also see supplemental data on MS fragments concerning sequence coverage of α-synuclein and fragment spectra from sumoylated α-synuclein tryptic peptides).

In vitro fibrillation assay

Recombinant human WT– and SUMO–modified α-synuclein solutions were dialysed against 50 mM Hepes buffer with 100 mM NaCl at pH 7.4. To remove any potential seed before aggregation, samples were centrifuged for 2 h at 100,000 *g* at 4°C. Protein concentration was adjusted to 70 µM. 0.01% of sterile, filtered NaN₃ was included in the aggregation mixtures, which were then incubated in glass vials at 37°C with constant stirring at 200 rpm. For ThioT fluorescence measurements, 5-µl aliquots were withdrawn from α-synuclein incubations and added to 2 ml of 5 µM ThioT in 50 mM glycine-NaOH, pH 8.2. Fluorescence measurements were performed on a spectrofluorometer (Cary Eclipse; Varian) using 3.5-ml quartz cuvettes (Hellma Analytics) with a path length of 1 cm. Fluorescence emission spectra were recorded from 465 to 600 nm using an excitation wavelength of 446 nm, an integration time of 0.1 s, and both excitation and emission bandwidths of 10 nm. Kinetic aggregation traces were generated from time traces of ThioT fluorescence intensity at 482 nm and corrected for free ThioT fluorescence. Data were normalized to the controls.

TEM

For negative staining, a solution containing protein was applied to glow-discharged, carbon-coated grids and stained with 1% uranyl acetate. Images were taken in an electron microscope (CM120; Philips) at a defocus of 2.3 µm using a slow-scan charge-coupled device camera (TemCam 224A; Tietz Video and Image Processing Systems).

PDZ assay

WT α-synuclein or 2KR (K96 and 102R) was tagged with a six–amino acid PDZ binding motif (HSTTRV from neuroligin 1) and coexpressed with the corresponding PDZ domain (PDZ1 domain of synaptic scaffolding molecule) fused to GFP. To ensure equal expression levels and eliminate differences in transfection efficiencies, WT α-synuclein and mutant tagged with the PDZ binding motif were subcloned in a bicistronic plasmid together with PDZ domain–GFP fusion under the same promoter (cytomegalovirus). HEK293T cells were Lipofectamine transfected with WT α-synuclein or 2KR and 2A mutants and fixed 36 h after transfection. Cell counts were obtained manually. The advantage of this approach is that a fluorescent protein is not directly fused to α-synuclein, and, at the same time, inclusions formed by α-synuclein can be fluorescently labeled via the PDZ binding motif (Opazo et al., 2008).

Viral vector production

rAAV2 were used as gene delivery vehicles of EGFP, WT α-synuclein, and α-synuclein–2KR (K96R and K102R). Transgene expression was controlled by the highly neuron-specific human synapsin 1 (hSyn1) promoter (Kügler et al., 2001). Viral vectors were propagated in 293T cells using the pDG2 helper plasmid (Grimm et al., 1998). Viral particles were purified according to established protocols (Zolotukhin et al., 1999) by iodixanol step gradient centrifugation. Samples were purified and concentrated by heparin affinity chromatography on an ÄKTA fast protein LC system using 1-ml HiTrap Heparin QFF columns (GE Healthcare) and desalted overnight by dialysis against PBS. Vector genomes were titrated by quantitative PCR. The purity of preparations was confirmed by SDS gel electrophoresis and silver staining.

Animal procedures

All experimental animal procedures were performed according to experimental licenses issued by the responsible animal welfare authority of Niedersächsisches Landesamt für Verbraucherschutz und Lebensmittelsicherheit and controlled by the local animal welfare committee of the University of Göttingen. Intracerebral stereotaxic injections into SN of 2.5-mo-old female Wistar rats, sacrifice, and perfusion were performed essentially as previously described (Shevtsova et al., 2006). In brief, vector injections into SNpc were performed using a Kopf stereotaxic device with a computer-controlled microinjector pump (Word Precision Instruments). Coordinates were as follows: anterior–posterior distance, −0.53; mediolateral distance, 0.22; and dorsoventral distance, −0.78, relative to bregma. A fine-bore glass capillary (30-µm diameter) was used to deliver the viral suspension.

Immunohistochemistry

PFA-perfused rat brains were frozen at −80°C and cut on a cryostat (CM 3050 S; Leica) to 30-µm coronary sections. The brain sections were shortly washed with PBS-T (0.1% Triton X-100 in PBS) and incubated in a blocking solution (10% FCS and 0.1% Triton X-100 in PBS) for 1 h at RT to avoid unspecific binding of the antibodies. Incubation with primary antibody (anti–α-synuclein, 1:1,000 [32-8100; Invitrogen]; anti-VMAT2, 1:3,000 [AB1767; Millipore]; and anti-NeuN, 1:300 [MAB377; Millipore]) was performed overnight at 4°C in PBS with 0.1% Triton X-100 and 2% normal goat serum. After washing with PBS, the secondary Cy2- and Cy3-coupled antibodies (1:250 in PBS with 0.1% Triton X-100 and 2% normal goat serum) were applied for 1 h at RT. The unbound secondary antibodies were washed out, and sections were mounted on microscope slides (SuperFrost Plus; Thermo Fisher Scientific), embedded in polyvinyl alcohol mounting medium with DABCO (Fluca), coated by coverslips, and kept at 4°C until microscopy.

Microscope image acquisition

Wide-field fluorescent images were obtained at RT using an Axioplan2 microscope equipped with a 5× LD Achroplan (Carl Zeiss) or 63× NA 1.4 oil objective (Carl Zeiss). The camera used was an AxioCam (Carl Zeiss), and Axiovision 4.7 (Carl Zeiss) was used as acquisition software.

Quantification of VMAT/NeuN-positive neurons in the SNpc

The number of VMAT- or NeuN-positive neurons in the SNpc was assessed using stereological methodology (West, 1999). Every third section was immunostained, and VMAT- or NeuN-positive neurons in the SNpc were counted from the left AAV2-injected side from a minimum of six animals per group using the optical dissector technique (Dehmer et al., 2004). The stereological quantification was performed using the Imager M2 microscope (Carl Zeiss). The software used was Stereo Investigator 6.0 (MicroBright-Field, Inc.). Counts were performed manually and blinded for treatment. Statistical evaluation was performed with KyPlot 5.0 software (KyensLab Inc.) using Student's *t* test.

References

Baba, D., N. Maita, J.G. Jee, Y. Uchimura, H. Saitoh, K. Sugasawa, F. Hanaoka, H. Tochio, H. Hiroaki, and M. Shirakawa. 2005. Crystal structure of thymine DNA glycosylase conjugated to SUMO-1. *Nature*. 435:979–982. doi:10.1038/nature03634

Bayer, P., A. Arndt, S. Metzger, R. Mahajan, F. Melchior, R. Jaenicke, and J. Becker. 1998. Structure determination of the small ubiquitin-related modifier SUMO-1. *J. Mol. Biol.* 280:275–286. doi:10.1006/jmbi.1998.1839

Bertoncini, C.W., Y.S. Jung, C.O. Fernandez, W. Hoyer, C. Griesinger, T.M. Jovin, and M. Zweckstetter. 2005. Release of long-range tertiary interactions potentiates aggregation of natively unstructured alpha-synuclein. *Proc. Natl. Acad. Sci. USA*. 102:1430–1435. doi:10.1073/pnas.0407146102

Bossis, G., and F. Melchior. 2006. SUMO: regulating the regulator. *Cell Div.* 1:13. doi:10.1186/1747-1028-1-13

Chandra, S., F. Fornai, H.B. Kwon, U. Yazdani, D. Atasoy, X. Liu, R.E. Hammer, G. Battaglia, D.C. German, P.E. Castillo, and T.C. Südhof. 2004. Double-knockout mice for alpha- and beta-synucleins: effect on synaptic functions. *Proc. Natl. Acad. Sci. USA*. 101:14966–14971. doi:10.1073/pnas.0406283101

Chandra, S., G. Gallardo, R. Fernández-Chacón, O.M. Schlüter, and T.C. Südhof. 2005. Alpha-synuclein cooperates with CSPalpha in preventing neurodegeneration. *Cell*. 123:383–396. doi:10.1016/j.cell.2005.09.028

Chang, T.H., T. Kubota, M. Matsuoka, S. Jones, S.B. Bradfute, M. Bray, and K. Ozato. 2009. Ebola Zaire virus blocks type I interferon production by exploiting the host SUMO modification machinery. *PLoS Pathog.* 5:e1000493. doi:10.1371/journal.ppat.1000493

Cimarosti, H., and J.M. Henley. 2008. Investigating the mechanisms underlying neuronal death in ischemia using in vitro oxygen-glucose deprivation: potential involvement of protein SUMOylation. *Neuroscientist*. 14:626–636. doi:10.1177/1073858408322677

Cimarosti, H., C. Lindberg, S.F. Bomholt, L.C. Rønn, and J.M. Henley. 2008. Increased protein SUMOylation following focal cerebral ischemia. *Neuropharmacology*. 54:280–289. doi:10.1016/j.neuropharm.2007.09.010

Crowther, R.A., S.E. Daniel, and M. Goedert. 2000. Characterisation of isolated alpha-synuclein filaments from substantia nigra of Parkinson's disease brain. *Neurosci. Lett.* 292:128–130. doi:10.1016/S0304-3940(00)01440-3

Dedmon, M.M., J. Christodoulou, M.R. Wilson, and C.M. Dobson. 2005. Heat shock protein 70 inhibits alpha-synuclein fibril formation via preferential binding to prefibrillar species. *J. Biol. Chem.* 280:14733–14740. doi:10.1074/jbc.M413024200

Dehmer, T., M.T. Heneka, M. Sastre, J. Dichgans, and J.B. Schulz. 2004. Protection by pioglitazone in the MPTP model of Parkinson's disease correlates with I kappa B alpha induction and block of NF kappa B and iNOS activation. *J. Neurochem.* 88:494–501. doi:10.1046/j.1471-4159.2003.02210.x

Dorval, V., and P.E. Fraser. 2006. Small ubiquitin-like modifier (SUMO) modification of natively unfolded proteins tau and alpha-synuclein. *J. Biol. Chem.* 281:9919–9924. doi:10.1074/jbc.M510127200

Duda, J.E., V.M. Lee, and J.Q. Trojanowski. 2000. Neuropathology of synuclein aggregates. *J. Neurosci. Res.* 61:121–127. doi:10.1002/1097-4547(20000715)61:2<121::AID-JNR1>3.0.CO;2-4

Fei, E., N. Jia, M. Yan, Z. Ying, Q. Sun, H. Wang, T. Zhang, X. Ma, H. Ding, X. Yao, et al. 2006. SUMO-1 modification increases human SOD1 stability and aggregation. *Biochem. Biophys. Res. Commun.* 347:406–412. doi:10.1016/j.bbrc.2006.06.092

Fujiwara, H., M. Hasegawa, N. Dohmae, A. Kawashima, E. Masliah, M.S. Goldberg, J. Shen, K. Takio, and T. Iwatsubo. 2002. alpha-Synuclein is phosphorylated in synucleinopathy lesions. *Nat. Cell Biol.* 4:160–164. doi:10.1038/ncb841

Fukae, J., Y. Mizuno, and N. Hattori. 2007. Mitochondrial dysfunction in Parkinson's disease. *Mitochondrion*. 7:58–62. doi:10.1016/j.mito.2006.12.002

Geiss-Friedlander, R., and F. Melchior. 2007. Concepts in sumoylation: a decade on. *Nat. Rev. Mol. Cell Biol.* 8:947–956. doi:10.1038/nrm2293

Giasson, B.I., J.E. Duda, I.V. Murray, Q. Chen, J.M. Souza, H.I. Hurtig, H. Ischiropoulos, J.Q. Trojanowski, and V.M. Lee. 2000. Oxidative damage linked to neurodegeneration by selective alpha-synuclein nitration in synucleinopathy lesions. *Science*. 290:985–989. doi:10.1126/science.290.5493.985

Grimm, D., A. Kern, K. Rittner, and J.A. Kleinschmidt. 1998. Novel tools for production and purification of recombinant adenoassociated virus vectors. *Hum. Gene Ther.* 9:2745–2760. doi:10.1089/hum.1998.9.18-2745

Hardeland, U., R. Steinacher, J. Jiricny, and P. Schär. 2002. Modification of the human thymine-DNA glycosylase by ubiquitin-like proteins facilitates enzymatic turnover. *EMBO J.* 21:1456–1464. doi:10.1093/emboj/21.6.1456

Hay, R.T. 2005. SUMO: a history of modification. *Mol. Cell.* 18:1–12. doi:10.1016/j.molcel.2005.03.012

Heise, H., W. Hoyer, S. Becker, O.C. Andronesi, D. Riedel, and M. Baldus. 2005. Molecular-level secondary structure, polymorphism, and dynamics of full-length alpha-synuclein fibrils studied by solid-state NMR. *Proc. Natl. Acad. Sci. USA*. 102:15871–15876. doi:10.1073/pnas.0506109102

Hsiao, H.H., E.E. Meulmeester, B.T. Frank, F. Melchior, and H. Urlaub. 2009. "ChopNSpice," a mass spectrometric approach that allows identification of endogenous small ubiquitin-like modifier-conjugated peptides. *Mol. Cell. Proteomics*. 8:2664–2675. doi:10.1074/mcp.M900087-MCP200

Irvine, G.B., O.M. El-Agnaf, G.M. Shankar, and D.M. Walsh. 2008. Protein aggregation in the brain: the molecular basis for Alzheimer's and Parkinson's diseases. *Mol. Med.* 14:451–464. doi:10.2119/2007-00100.Irvine

Iwai, A., E. Masliah, M. Yoshimoto, N. Ge, L. Flanagan, H.A. de Silva, A. Kittel, and T. Saitoh. 1995. The precursor protein of non-A beta component of Alzheimer's disease amyloid is a presynaptic protein of the central nervous system. *Neuron*. 14:467–475. doi:10.1016/0896-6273(95)90302-X

Jaffray, E.G., and R.T. Hay. 2006. Detection of modification by ubiquitin-like proteins. *Methods*. 38:35–38. doi:10.1016/j.ymeth.2005.07.020

Janer, A., A. Werner, J. Takahashi-Fujigasaki, A. Daret, H. Fujigasaki, K. Takada, C. Duyckaerts, A. Brice, A. Dejean, and A. Sittler. 2010. SUMOylation attenuates the aggregation propensity and cellular toxicity of the polyglutamine expanded ataxin-7. *Hum. Mol. Genet.* 19:181–195. doi:10.1093/hmg/ddp478

Johnson, E.S. 2004. Protein modification by SUMO. *Annu. Rev. Biochem.* 73:355–382. doi:10.1146/annurev.biochem.73.011303.074118

Kindsmüller, K., P. Groitl, B. Härtl, P. Blanchette, J. Hauber, and T. Dobner. 2007. Intranuclear targeting and nuclear export of the adenovirus E1B-55K protein are regulated by SUMO1 conjugation. *Proc. Natl. Acad. Sci. USA*. 104:6684–6689. doi:10.1073/pnas.0702158104

Krüger, R., W. Kuhn, T. Müller, D. Woitalla, M. Graeber, S. Kösel, H. Przuntek, J.T. Epplen, L. Schöls, and O. Riess. 1998. Ala30Pro mutation in the gene encoding alpha-synuclein in Parkinson's disease. *Nat. Genet.* 18:106–108. doi:10.1038/ng0298-106

Kügler, S., L. Meyn, H. Holzmüller, E. Gerhardt, S. Isenmann, J.B. Schulz, and M. Bähr. 2001. Neuron-specific expression of therapeutic proteins: evaluation of different cellular promoters in recombinant adenoviral vectors. *Mol. Cell. Neurosci.* 17:78–96. doi:10.1006/mcne.2000.0929

Marblestone, J.G., S.C. Edavettal, Y. Lim, P. Lim, X. Zuo, and T.R. Butt. 2006. Comparison of SUMO fusion technology with traditional gene fusion systems: enhanced expression and solubility with SUMO. *Protein Sci.* 15:182–189. doi:10.1110/ps.051812706

Miake, H., H. Mizusawa, T. Iwatsubo, and M. Hasegawa. 2002. Biochemical characterization of the core structure of alpha-synuclein filaments. *J. Biol. Chem.* 277:19213–19219. doi:10.1074/jbc.M110551200

Miller, D.W., S.M. Hague, J. Clarimon, M. Baptista, K. Gwinn-Hardy, M.R. Cookson, and A.B. Singleton. 2004. Alpha-synuclein in blood and brain from familial Parkinson disease with SNCA locus triplication. *Neurology*. 62:1835–1838.

Mukherjee, S., M. Thomas, N. Dadgar, A.P. Lieberman, and J.A. Iñiguez-Lluhí. 2009. Small ubiquitin-like modifier (SUMO) modification of the androgen receptor attenuates polyglutamine-mediated aggregation. *J. Biol. Chem.* 284:21296–21306. doi:10.1074/jbc.M109.011494

Opazo, F., A. Krenz, S. Heermann, J.B. Schulz, and B.H. Falkenburger. 2008. Accumulation and clearance of alpha-synuclein aggregates demonstrated by time-lapse imaging. *J. Neurochem.* 106:529–540. doi:10.1111/j.1471-4159.2008.05407.x

Palacios, S., L.H. Perez, S. Welsch, S. Schleich, K. Chmielarska, F. Melchior, and J.K. Locker. 2005. Quantitative SUMO-1 modification of a vaccinia virus protein is required for its specific localization and prevents its self-association. *Mol. Biol. Cell*. 16:2822–2835. doi:10.1091/mbc.E04-11-1005

Panavas, T., C. Sanders, and T.R. Butt. 2009. SUMO fusion technology for enhanced protein production in prokaryotic and eukaryotic expression systems. *Methods Mol. Biol.* 497:303–317. doi:10.1007/978-1-59745-566-4_20

Polymeropoulos, M.H., C. Lavedan, E. Leroy, S.E. Ide, A. Dehejia, A. Dutra, B. Pike, H. Root, J. Rubenstein, R. Boyer, et al. 1997. Mutation in the alpha-synuclein gene identified in families with Parkinson's disease. *Science*. 276:2045–2047. doi:10.1126/science.276.5321.2045

Sapetschnig, A., G. Rischitor, H. Braun, A. Doll, M. Schergaut, F. Melchior, and G. Suske. 2002. Transcription factor Sp3 is silenced through SUMO modification by PIAS1. *EMBO J.* 21:5206–5215. doi:10.1093/emboj/cdf510

Serpell, L.C., J. Berriman, R. Jakes, M. Goedert, and R.A. Crowther. 2000. Fiber diffraction of synthetic alpha-synuclein filaments shows amyloid-like cross-beta conformation. *Proc. Natl. Acad. Sci. USA*. 97:4897–4902. doi:10.1073/pnas.97.9.4897

Shevtsova, Z., I. Malik, M. Garrido, U. Schöll, M. Bähr, and S. Kügler. 2006. Potentiation of in vivo neuroprotection by BclX(L) and GDNF co-expression depends on post-lesion time in deafferentiated CNS neurons. *Gene Ther.* 13:1569–1578. doi:10.1038/sj.gt.3302822

Shimura, H., M.G. Schlossmacher, N. Hattori, M.P. Frosch, A. Trockenbacher, R. Schneider, Y. Mizuno, K.S. Kosik, and D.J. Selkoe. 2001. Ubiquitination of a new form of alpha-synuclein by parkin from human brain: implications for Parkinson's disease. *Science*. 293:263–269. doi:10.1126/science.1060627

Singleton, A.B., M. Farrer, J. Johnson, A. Singleton, S. Hague, J. Kachergus, M. Hulihan, T. Peuralinna, A. Dutra, R. Nussbaum, et al. 2003. alpha-Synuclein locus triplication causes Parkinson's disease. *Science*. 302:841. doi:10.1126/science.1090278

Steffan, J.S., N. Agrawal, J. Pallos, E. Rockabrand, L.C. Trotman, N. Slepko, K. Illes, T. Lukacsovich, Y.Z. Zhu, E. Cattaneo, et al. 2004. SUMO modification of Huntingtin and Huntington's disease pathology. *Science*. 304:100–104. doi:10.1126/science.1092194

Uchimura, Y., M. Nakamura, K. Sugasawa, M. Nakao, and H. Saitoh. 2004. Overproduction of eukaryotic SUMO-1- and SUMO-2-conjugated proteins in *Escherichia coli*. *Anal. Biochem.* 331:204–206.

Vilar, M., H.T. Chou, T. Lührs, S.K. Maji, D. Riek-Loher, R. Verel, G. Manning, H. Stahlberg, and R. Riek. 2008. The fold of alpha-synuclein fibrils. *Proc. Natl. Acad. Sci. USA*. 105:8637–8642. doi:10.1073/pnas.0712179105

Werner, A., M.C. Moutty, U. Möller, and F. Melchior. 2009. Performing in vitro sumoylation reactions using recombinant enzymes. *Methods Mol. Biol.* 497:187–199. doi:10.1007/978-1-59745-566-4_12

West, M.J. 1999. Stereological methods for estimating the total number of neurons and synapses: issues of precision and bias. *Trends Neurosci.* 22:51–61. doi:10.1016/S0166-2236(98)01362-9

Wilkinson, K.A., and J.M. Henley. 2010. Mechanisms, regulation and consequences of protein SUMOylation. *Biochem. J.* 428:133–145. doi:10.1042/BJ20100158

Yang, W., H. Sheng, D.S. Warner, and W. Paschen. 2008. Transient global cerebral ischemia induces a massive increase in protein sumoylation. *J. Cereb. Blood Flow Metab.* 28:269–279. doi:10.1038/sj.jcbfm.9600523

Zarranz, J.J., J. Alegre, J.C. Gómez-Esteban, E. Lezcano, R. Ros, I. Ampuero, L. Vidal, J. Hoenicka, O. Rodriguez, B. Atarés, et al. 2004. The new mutation, E46K, of alpha-synuclein causes Parkinson and Lewy body dementia. *Ann. Neurol.* 55:164–173. doi:10.1002/ana.10795

Zhou, C., Y. Huang, and S. Przedborski. 2008. Oxidative stress in Parkinson's disease: a mechanism of pathogenic and therapeutic significance. *Ann. NY Acad. Sci.* 1147:93–104. doi:10.1196/annals.1427.023

Zolotukhin, S., B.J. Byrne, E. Mason, I. Zolotukhin, M. Potter, K. Chesnut, C. Summerford, R.J. Samulski, and N. Muzyczka. 1999. Recombinant adeno-associated virus purification using novel methods improves infectious titer and yield. *Gene Ther.* 6:973–985. doi:10.1038/sj.gt.3300938